Enhanced Optical Performance of AlGaN-Based Deep Ultraviolet Light-Emitting Diodes by Electrode Patterns Design

Qian Chen, Jiangnan Dai, Xiaohang Li, *Member, IEEE*, Yang Gao, Hanling Long, Zi-Hui Zhang, Changqing Chen, *Member, IEEE*, and Hao-Chung Kuo, *Fellow, IEEE*

***Abstract*— Low external quantum efficiency of deep ultraviolet light-emitting diodes (DUV LEDs) and current crowding can result in considerable heat generation, which has a great negative impact on device performance. In this paper, we investigate the influence of different electrode patterns on the photoelectric and thermal performance of DUV LEDs. We find that different electrode designs can achieve drastically different optical powers, with the superior design being the n-type electrode surrounding the active region. Moreover, compared with the counterpart, the superior design does not affect the electrical performance. The main reason is that the N-surrounding electrode pattern can provide enough current paths for carrier transport, thus realizing a more uniform current injection and can further improve the external quantum efficiency for DUV LEDs.**

***Index Terms*— DUV LEDs, PN electrode location, current spreading.**

I. Introduction

BECAUSE of enormous application potentials in critical fields such as air purification, water sterilization, and communication, AlGaN-based deep ultraviolet light emitting diodes (DUV LEDs) have attracted increasing attention [1]–[3]. However, current crowding along with higher-resistivity Al-rich AlGaN layers can lead to large heat generation, reduced device lifetime, and limited external quantum efficiency (EQE) [4], [5]. Therefore, the design of device architecture has a significant impact on the device performance besides the improvement of epitaxial wafer crystal quality for higher radiative efficiency [6]–[10].

Previously, deliberate electrode pattern designs have been shown to effectively improve current spreading, reduce junction temperature, enable better device performance, and extend the lifetime of InGaN-based visible LEDs and AlGaN-based DUV LEDs [11]–[15]. For instance, Guo *et al.* investigated and optimized the interdigital electrode pattern of visible LEDs, which achieves improved electrical performance [13]. However, the shortcoming is the increased total distance of the edge of interdigital electrode when comparing with the square electrode pattern, and this can lead to more leakage current. Horng *et al.* further evolved the interdigital electrode to the hole-shaped electrode to obtain the uniform current spreading and better light output power for visible LEDs [14]. Zhang *et al.* applied the hole-shaped electrode to DUV LEDs, and realized similar benefits [15]. Thus far, significant attention has been made to the shape and the size of the electrode, while few reports have been published to uncover the impacts of the PN electrode location on the current transport and device characteristics, especially for DUV LEDs.

In this work, we have investigated two opposite PN electrode locations: the N-surrounding electrode pattern, i.e., the active region is surrounded by the N-electrode at the edge; and the P-surrounding electrode pattern, i.e., the N-electrode locates at the center of LED surrounded by the active region. We find that the N-surrounding electrode pattern can well manage the layer resistance and better modulate the current paths, thus homogenizing the current spreading and enhancing the EQE for DUV LEDs.

II. Experiments

As shown in Fig. 1(a), the DUV LEDs were grown on *c*-plane sapphire substrates by metalorganic chemical vapor deposition (MOCVD) [16]. We firstly grew a 1.5-μm-thick AlN buffer layer on the sapphire substrate, followed by a 3-μm-thick Si-doped n-type AlGaN contact layer, for which the doping concentration is $\sim 5\times10^{18}$ cm^{-3}. Then the

Manuscript received October 6, 2019; revised October 17, 2019; accepted October 18, 2019. Date of publication October 22, 2019; date of current version November 27, 2019. This work was supported in part by the National Key Research and Development Program of China under Grant 2018YFB0406602, and in part by the National Natural Science Foundation of China under Grant 11574166, Grant 61377034, and Grant 61774065. The review of this letter was arranged by Editor O. Manasreh. *(Corresponding author: Jiangnan Dai.)*

Q. Chen, J. Dai, Y. Gao, H. Long, and C. Chen are with the Wuhan National Laboratory for Optoelectronics, Huazhong University of Science and Technology, Wuhan 430074, China (e-mail: daijiangnan@hust.edu.cn).

X. Li is with the Advanced Semiconductor Laboratory, King Abdullah University of Science and Technology, Thuwal 23955, Saudi Arabia.

Z.-H. Zhang is with the State Key Laboratory of Reliability and Intelligence of Electrical Equipment, Tianjin 300401, China.

H.-C. Kuo is with the Department of Photonics and Institute of Electro-Optical Engineering, National Chiao Tung University, Hsinchu 30010, Taiwan.

Color versions of one or more of the figures in this letter are available online at http://ieeexplore.ieee.org.

Digital Object Identifier 10.1109/LED.2019.2948952

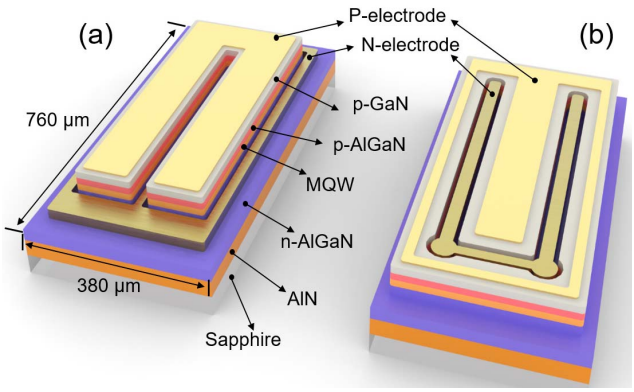

Fig. 1. Schematic diagrams of DUV LEDs with (a) the N-surrounding electrode pattern and (b) the P-surrounding electrode pattern.

following active region includes five 3-nm-thick $Al_{0.45}Ga_{0.55}N$ quantum wells separated by six 10-nm-thick $Al_{0.55}Ga_{0.45}N$ barriers, emitting at 286 nm. A 25-nm-thick Mg-doped p-type electron blocking layer (EBL) is grown on the top of the active region, followed by a 50-nm-thick p-type Al-grading AlGaN layer and a 200-nm-thick p-type GaN contact layer with the Mg doping concentrations of 3×10^{19}, 8×10^{19}, and 1×10^{20} cm^{-3}, respectively. After the growth, the wafer was annealed for 30 minutes at 850 °C for Mg activation.

Subsequently, these two types of DUV LED chips are fabricated on the same epitaxy wafer by following the standard LED chip process we have developed [17], [18]. Firstly, we etch the epitaxial wafers according to the mesa pattern from the p-type GaN to the n-type AlGaN layer. Then the N-electrode of Cr/Al/Ti/Au (20/30/20/100 nm) stacks are deposited on the surface of n-type AlGaN by the electron beam evaporation, which is then annealed by rapid thermal annealing to form ohmic contact. The P-electrode comprises Ni/Au/Ni/Au (5/5/30/50 nm) metal stack. The chip size is the 380 μm $\times$760 μm. As shown in Figs.1(b) and (c), the electrode shapes are divided into N-surrounding and P-surrounding electrode patterns. The area of quantum well active regions for the two types of LED chips are different, which are 56% and 70% for N-surrounding and P-surrounding DUV LEDs, respectively, of the individual chip. The edges of all N-electrode are controlled at the distance of 10 μm from edges of mesa to facilitate the subsequent process, as well as the P-electrode. These chips were packaged on the AlN ceramic carriers with eutectic technology for subsequent temperature and electroluminescence measurements [19].

III. Results and Discussion

The electrical and optical characteristics of the N-surrounding and P-surrounding DUV LEDs are measured at room temperature with CW current. Fig. 2 (a) shows that both devices have almost identical turn-on voltage and IV characteristics, indicating similar input power at any given forward current. Fig. 2(b) illustrates that the N-surrounding DUV-LED has a considerably higher optical power than that of the P-surrounding DUV LED. For instance, the enhancement is 41.0% at injection current of 100 mA,

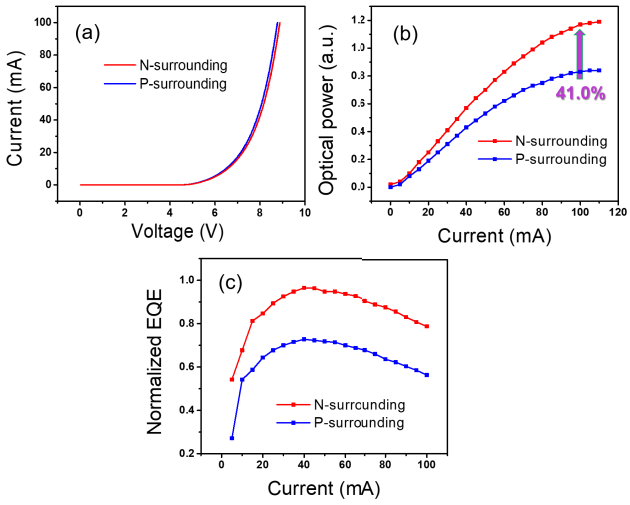

Fig. 2. (a) Forward current versus voltage for the two DUV LEDs. (b) Relative optical power and (c) normalized EQE versus the current for the two DUV LEDs.

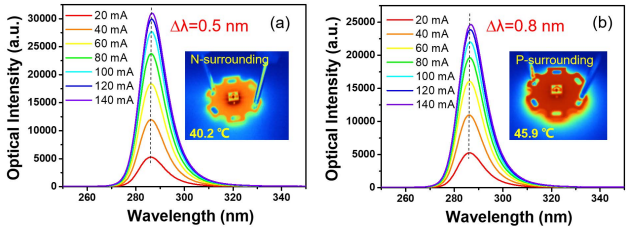

Fig. 3. The spectra of (a) the N-surrounding DUV-LED and (b) the P-surrounding DUV-LED from 20 to 140 mA, the red-shifts of the peak wavelength are 0.5 and 0.8 nm, respectively in (a) and (b). The inset thermal images of N-surrounding and P-surrounding are test at 100 mA.

even though the emitting area of the N-surrounding device is only 80% (56%/70%) of that of the P-surrounding device. The enhanced optical power translates to higher EQE in Fig. 2(c) where the normalized EQE is shown with respect to the EQE of the N-surrounding DUV LED. We also calculate the efficiency droop levels at 100 mA, which are 17.9% and 22.8% for the N-surrounding and P-surrounding DUV LEDs, respectively, down from the maximum EQEs. Therefore, the N-surrounding DUV LED exhibits less efficiency droop.

Most input power not converted into photos turns into thermal energy, which could lead to detrimental impacts on the device performance and lifetime. Thus, we perform the measurement of the surface temperature of the two DUV LEDs operating at 100 mA by an infrared thermal imaging system (Fluke Ti32) shown in the inset of Figs. 3(a) and (b). We find that the working temperature of the P-surrounding DUV-LED reaches 45.9 °C, which is more than five degrees higher than that of the N-surrounding DUV LED of 40.2 °C. According to the study by Park *et al.*, a similar junction temperature increase can lead to considerable reduction of IQE or EQE [20]. The observations here mean that less power is wasted on heat generation for the N-surrounding DUV LED. Thanks to the less generated heat, the red-shift level of peak wavelength for the N-surrounding LED is smaller as the increasing injection current level [21], [22], which can be

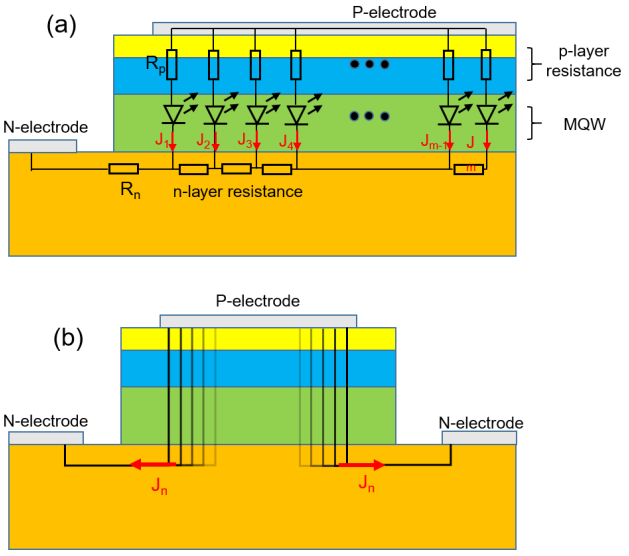

Fig. 4. (a) Schematic diagrams of simplified current circuit at the edge of mesa, (b) simplified current transport paths in the LED.

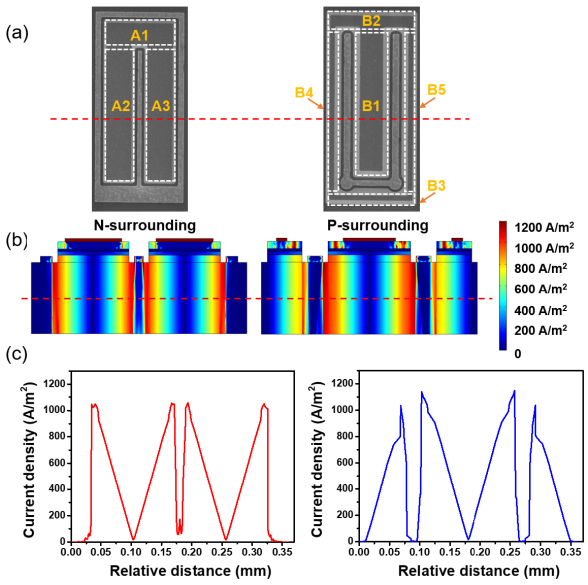

Fig. 5. (a) Scanning electron microscopy (SEM) images for N-surrounding and P-surrounding DUV LEDs, (b) 2D simulated current density profiles along the red line in the Fig. (a), (c) 1D simulated current density profiles along the red line in the Fig. (b).

seen in Figs. 3 (a) and (b). The improved performance for the N-surrounding DUV LED can be attributed to more superior current spreading, which is discussed as follows.

The current spreading is strongly affected by the layer resistivity for DUV LEDs. Thus, Fig. 4(a) sketches the circuits for a conventional DUV LED, where metal is used as electrodes. Since the metal has an extremely low resistivity as opposed to the p-type semiconductors, Fig. 4(b) indicates that the current crowding effect takes place on the edge of metal current spreading layer [23]. Moreover, the significant current crowding can also be predicted at the edge of the N-electrode. Our speculations are further proven by referring to Fig. 4(d), which shows the current crowding at the edge of the N-electrode. Besides, there is a current accumulation at the edge of the P-electrode [24]. The nonuniform current distribution can accordingly degrade the carrier injection and increase the device temperature.

Fig. 5(a) shows the division of the N-surrounding and P-surrounding DUV LED regions, in which the N-surrounding LED is divided into A1, A2, A3 three regions, and the P-surrounding LED is divided into B1, B2, B3, B4, B5 five regions. We can see intuitively that A1, A2 and A3 regions are surrounded by N-electrodes, and hence they have enough paths for carriers to transport. As shown in the schematic circuit diagram in Fig. 4(b), multi-side electrode wrapping enables carriers to be transported from different directions to N-electrode, which can effectively alleviate the current crowding effect in a single direction. In contrast, in the design of the P-surrounding electrodes, only B1 region has similar excellent current transmission paths, while the other regions i.e., B2, B3, B4, B5, are only adjacent to the N electrode on one side. Thus the carriers contributing to the luminescence in these regions cannot be effectively and rapidly transported to the N-electrode, which are easily accumulated at the edge of the mesa edge until congestion. Therefore, the N-surrounding LED has more superior electrode layout design, which enables greater carrier transport capability.

Through the finite element simulation analysis, we calculate the cross-sectional distribution of the current density at the position of red dotted line in Fig. 5(a) under the same injection current. As discussed earlier, the current accumulation at the edge of mesa is obvious, and a small part of the current accumulated at the edge of n-/p- electrodes. Furthermore, we extract the current density at the red dotted line in Fig. 5(b) and draw it in Fig. 5(c). It is illustrated that the LED with the P-surrounding electrodes has a higher current density than that with N-surrounding electrodes, which confirms the mechanism we discussed before. Meanwhile, it is also proven that the electrode pattern design has a profound effect on the DUV LED performance.

IV. Conclusion

In this work, the performance of 286 nm DUV-LEDs with different electrode patterns has been investigated. The device with the N-surrounding electrode shows significantly better overall performance with the stronger optical power, lower working temperature, and smaller wavelength shift than the P-surrounding DUV LED. The improved performance is mainly due to the enhanced current spreading effect. Our findings suggest that deliberate electrode patterns designs can improve and play a crucial role in the overall performance of the DUV LED chips and ought to be carefully investigated.

References

[1] M. Kneissl, T.-Y. Seong, J. Han, and H. Amano, "The emergence and prospects of deep-ultraviolet light-emitting diode technologies," *Nature Photon.*, vol. 13, no. 4, pp. 233–244, Apr. 2019. doi: 10.1038/s41566-019-0359-9.

[2] A. Khan, K. Balakrishnan, and T. Katona, "Ultraviolet light-emitting diodes based on group three nitrides," *Nature Photon.*, vol. 2, no. 2, pp. 77–84, Feb. 2008. doi: 10.1038/nphoton.2007.293.

[3] H. Hirayama, S. Fujikawa, N. Noguchi, J. Norimatsu, T. Takano, K. Tsubaki, and N. Kamata, "222–282 nm AlGaN and InAlGaN-based deep-UV LEDs fabricated on high-quality AlN on sapphire," *Phys. Status Solidi A*, vol. 206, no. 6, pp. 1176–1182, Jun. 2009. doi: 10.1002/pssa.200880961.

[4] M. Shatalov, W. Sun, R. Jain, A. Lunev, X. Hu, A. Dobrinsky, Y. Bilenko, J. Yang, G. A. Garrett, L. E. Rodak, M. Wraback, M. Shur, and R. Gaska, "High power AlGaN ultraviolet light emitters," *Semicond. Sci. Technol.*, vol. 29, no. 8, Aug. 2014, Art. no. 084007. doi: 10.1088/0268-1242/29/8/084007.

[5] S. C. Mangham, J. Wu, S. Lee, V. R. Reddy, and O. Manasreh, "Surface plasmon enhanced photoluminescence in InAs quantum dots by spherical Ag nanoparticles," *MRS Online Proc. Library Arch.*, vol. 1391, Apr. 2012. doi: 10.1557/opl.2012.692.

[6] K. Xu, Y. Chen, T. A. Okhai, and L. W. Snyman, "Micro optical sensors based on avalanching silicon light-emitting devices monolithically integrated on chips," *Opt. Mater. Express*, vol. 9, no. 10, pp. 3985–3997, Oct. 2019. doi: 10.1364/OME.9.003985.

[7] T. Takano, T. Mino, J. Sakai, N. Noguchi, K. Tsubaki, and H. Hirayama, "Deep-ultraviolet light-emitting diodes with external quantum efficiency higher than 20% at 275 nm achieved by improving light-extraction efficiency," *Appl. Phys. Express*, vol. 10, no. 3, 2017, Art. no. 031002. doi: 10.7567/APEX.10.031002.

[8] Y. A. Guo, Y. Zhang, J. Yan, H. Xie, L. Liu, X. Chen, M. Hou, Z. Qin, J. Wang, and J. Li, "Light extraction enhancement of AlGaN-based ultraviolet light-emitting diodes by substrate sidewall roughening," *Appl. Phys. Lett.*, vol. 111, no. 1, Jul. 2017, Art. no. 011102. doi: 10.1063/1.4991664.

[9] H. Chang, Z. Chen, W. Li, J. Yan, R. Hou, S. Yang, Z. Liu, G. Yuan, J. Wang, J. Li, P. Gao, and T. Wei, "Graphene-assisted quasi-van der Waals epitaxy of AlN film for ultraviolet light emitting diodes on nano-patterned sapphire substrate," *Appl. Phys. Lett*, vol. 114, no. 9, Mar. 2019, Art. no. 091107. doi: 10.1063/1.5081112.

[10] W. Guo, S. Mitra, J. Jiang, H. Xu, M. Sheikhi, H. Sun, K. Tian, Z.-H. Zhang, H. Jiang, I. S. Roqan, X. Li, and J. Ye, "Three-dimensional band diagram in lateral polarity junction III-nitride heterostructures," *Optica*, vol. 6, no. 8, pp. 1058–1062, Aug. 2019. doi: 10.1364/OPTICA.6.001058.

[11] V. K. Malyutenko, S. S. Bolgov, and A. D. Podoltsev, "Current crowding effect on the ideality factor and efficiency droop in blue lateral InGaN/GaN light emitting diodes," *Appl. Phys. Lett.*, vol. 97, no. 25, Dec. 2010, Art. no. 251110. doi: 10.1063/1.3529470.

[12] S. Hwang and J. Shim, "A method for current spreading analysis and electrode pattern design in light-emitting diodes," *IEEE Trans. Electron Devices*, vol. 55, no. 5, pp. 1123–1128, May 2008. doi: 10.1109/TED.2008.918414.

[13] X. Guo, Y.-L. Li, and E. F. Schubert, "Efficiency of GaN/InGaN light-emitting diodes with interdigitated mesa geometry," *Appl. Phys. Lett.*, vol. 79, no. 13, pp. 1936–1938, Sep. 2001. doi: 10.1063/1.1405145.

[14] R.-H. Horng, S.-H. Chuang, C.-H. Tien, S.-C. Lin, and D.-S. Wuu, "High performance GaN-based flip-chip LEDs with different electrode patterns," *Opt. Express*, vol. 22, pp. A941–A946, May 2014. doi: 10.1364/OE.22.00A941.

[15] S. Zhang, F. Wu, S. Wang, H. Zhang, Y. Zhang, L. Xu, J. Dai, and C. Chen, "Enhanced wall-plug efficiency in AlGaN-based deep-ultraviolet LED via a novel honeycomb hole-shaped structure," *IEEE Trans. Electron Devices*, vol. 66, no. 7, pp. 2997–3002, Jul. 2019. doi: 10.1109/TED.2019.2913962.

[16] H. Long, F. Wu, J. Zhang, S. Wang, J. Chen, C. Zhao, Z. C. Feng, J. Xu, X. Li, J. Dai, and C. Chen, "Anisotropic optical polarization dependence on internal strain in AlGaN epilayer grown on Al_x Ga_{1-x} N templates," *J. Phys. D, Appl. Phys.*, vol. 49, no. 41, Sep. 2016, Art. no. 415103. doi: 10.1088/0022-3727/49/41/415103.

[17] Y. Gao, Q. Chen, S. Zhang, H. Long, J. Dai, H. Sun, and C. Chen, "Enhanced light extraction efficiency of AlGaN-based deep ultraviolet light-emitting diodes by incorporating high-reflective n-type electrode made of Cr/Al," *IEEE Trans. Electron Devices*, vol. 66, no. 7, pp. 2992–2996, Jul. 2019. doi: 10.1109/TED.2019.2914487.

[18] K. K. Xu, L. Huang, Z. Y. Zhang, J. M. Zhang, Z. P. Zhang, L. W. Snyman, and J. W. Swart, "Light emission from a poly-silicon device with carrier injection engineering," *Mater. Sci. Eng. B*, vol. 231, pp. 28–31, May 2018. doi: 10.1016/j.mseb.2018.07.002.

[19] R. Liang, J. Zhang, S. Wang, Q. Chen, L. Xu, J. N. Dai, and C. Chen, "Investigation on thermal characterization of eutectic flip-chip UV-LEDs with different bonding voidage," *IEEE Trans. Electron Devices*, vol. 64, no. 3, pp. 1174–1179, Mar. 2017. doi: 10.1109/TED.2017.2656240.

[20] J. Park and C. C. Lee, "An electrical model with junction temperature for light-emitting diodes and the impact on conversion efficiency," *IEEE Electron Device Lett.*, vol. 26, no. 5, pp. 308–310, May 2005. doi: 10.1109/LED.2005.847407.

[21] J. Senawiratne, A. Chatterjee, T. Detchprohm, W. Zhao, M. Zhu, Y. Xia, X. Li, J. Plawsky, and C. Wetzel, "Junction temperature, spectral shift, and efficiency in GaInN-based blue and green light emitting diodes," *Thin Solid Films*, vol. 518, no. 6, pp. 1732–1736, Jan. 2010. doi: 10.1016/j.tsf.2009.11.073.

[22] M. Du Plessis, H. Wen, and E. Bellotti, "Temperature characteristics of hot electron electroluminescence in silicon," *Opt. Express*, vol. 23, no. 10, pp. 12605–12612, May 2015. doi: 10.1364/OE.23.012605.

[23] K. Xu, "Silicon MOS optoelectronic micro-nano structure based on reverse-biased PN junction," *Phys. Status Solidi A*, vol. 216, no. 7, Apr. 2019, Art. no. 1800868. doi: 10.1002/pssa.201800868.

[24] Z.-H. Zhang, S. T. Tan, W. Liu, Z. G. Jun, K. Zheng, Z. Kyaw, Y. Ji, N. Hasanov, X. W. Sun, and H. V. Demir, "Improved InGaN/GaN light-emitting diodes with a p-GaN/n-GaN/p-GaN/n-GaN/p-GaN current-spreading layer," *Opt. Express*, vol. 21, no. 4, pp. 4958–4969, 2013. doi: 10.1364/OE.21.004958.